Not in one metric: Neuroticism modulates different resting state metrics within distinctive brain regions

Claudio Gentili1[1*], Ioana Alina Cristea[1,2*], Emiliano Ricciardi[3], Nicola Vanello[4], Cristian Popita[5], Daniel David[2] , Pietro Pietrini[3]

1. Department of General Psychology, University of Padua, Padua, Italy

2. Department of Clinical Psychology and Psychotherapy and International Institute for Advanced Studies of Psychotherapy and Applied Mental Health**,** University Babes-Bolyai, Cluj-Napoca, Romania.

3. IMT School for Advanced Studies Lucca, Italy

4. Dipartimento di Ingegneria dell'Informazione, University of Pisa, Italy

5. Department of Radiology, The Oncology Institute "Prof. Dr. Ion Chiricuta" (IOCN), Cluj-Napoca, Romania

Corresponding Author:

Claudio Gentili, M.D. Ph.D.

Associate Professor, Department of General Psychology, University of Padua, Via Venezia 8, Padua, Italy

c.gentili@unipd.it

* C.G. and I.C. had equal contributions for this manuscript.

Running Head: Neuroticism modulates resting activity metrics in distinctive regions

Abstract:

Introduction: Neuroticism is a complex personality trait encompassing diverse aspects. Notably, high levels of neuroticism are related to the onset of psychiatric conditions, including anxiety and mood disorders. Personality *traits* are stable individual features; therefore, they can be expected to be associated with stable neurobiological features, including the Brain Resting State (RS) activity as measured by fMRI. Several metrics have been used to describe RS properties, yielding rather inconsistent results. This inconsistency could be due to the fact that different metrics portray different RS signal properties and that these properties may be differently affected by neuroticism. To explore the distinct effects of neuroticism, we assessed several distinct metrics portraying different RS properties within the same population.

Method: Neuroticism was measured in 31 healthy subjects using the Zuckerman-Kuhlman Personality Questionnaire; RS was acquired by high-resolution fMRI. Using linear regression, we examined the modulatory effects of neuroticism on RS activity, as quantified by the Amplitude of low frequency fluctuations (ALFF, fALFF), regional homogeneity (REHO), Hurst Exponent (H), global connectivity (GC) and amygdalae functional connectivity.

Results: Neuroticism modulated the different metrics across a wide network of brain regions, including emotional regulatory, default mode and visual networks. Except for some similarities in key brain regions for emotional expression and regulation, neuroticism affected different metrics in different ways.

Discussion: Metrics more related to the measurement of regional intrinsic brain activity (fALFF, ALFF and REHO), or that provide a parsimonious index of integrated and segregated brain activity (HE), were more broadly modulated in regions related to emotions and their regulation. Metrics related to connectivity were modulated across a wider network of areas. Overall, these results show that neuroticism affects distinct aspects of brain resting state activity. More in general, these findings indicate that a multiparametric approach may be required to obtain a more detailed characterization of the neural underpinnings of a given psychological trait.

Key words: Neuroticism, fMRI, resting state, fALFF, Functional connectivity, brain activity

1. Introduction

Neuroticism is one of the fundamental traits in personality theories. Its core characteristics include emotional instability, along with depression and anxiety symptoms (Zuckerman, 2005; Zuckerman et al., 1993). Neuroticism is part of almost every modern personality assessment and model. Notably, neuroticism factors across different personality models tend to be highly correlated among each others (Zuckerman et al., 1999). Moreover, high neuroticism is associated with trait anxiety and represents a predictive index for the clinical onset of anxiety and mood disorders (Derryberry and Reed, 1994; Kendler et al., 2006; Kendler et al., 2004; Kotov et al., 2010; Weinstock and Whisman, 2006). Finally, neuroticism seems to play a role in maladaptive juvenile schemas that may lead to criminal acts (Daffern et al., 2015).

Several studies looked at how neuroticism modulates responses to emotional cues or stressors. A recent meta-analysis on 18 papers identified several brain regions in which neural activity was modulated by neuroticism in response to perception of negative emotional stimuli, as compared to neutral ones. In particular, areas involved in the anticipation of aversive stimuli - including anterior and posterior cingulate, and putamen - were negatively correlated with neuroticism, while those involved in fear learning and emotional regulation - including the median cingulate, the hippocampus and the superior frontal gyrus - were positively correlated (Servaas et al., 2013).

Studies of functional connectivity during tasks also offered important insights for the understanding of the neurobiology of neuroticism. During a face perception task, higher neuroticism was associated with increased functional connectivity between the right amygdala and the fusiform gyrus. Conversely, an opposite pattern was found in the left amygdala, whose connectivity strength with the anterior cingulate cortex was negatively related to neuroticism. This latter result suggests that

higher neuroticism may be related to a diminished control function of the cingulate over the amygdala while processing emotional stimuli (Cremers et al., 2010).

Recently, the study of resting state brain activity has been proposed as a novel way to identify neurobiological correlates of psychological traits (Barkhof et al., 2014; Damoiseaux et al., 2006; Deco et al., 2011; Pannekoek et al., 2013; Peterson et al., 2014). The rationale for studying brain neural activity at rest stems from the notion that since a trait is a stable aspect of personality, its effects should be detectable in a stable configuration of brain activity (Gentili et al., 2015). In other words, while the modulatory effects on neural activity due to a *state* condition may be expressed maximally only when such a condition is elicited by an *ad-hoc* experimental paradigm, modulatory effects of a *trait* feature should affect brain activity permanently (Gentili et al., 2015).

Several metrics have been developed to study the brain resting state activity. Among them, Regional Homogenity (REHO), functional connectivity and measures of low frequency oscillation (LFO), including the Amplitude of Low Frequency Fluctuations – ALFF – and the fractional Amplitude of Low Frequency Fluctuations – fALFF, were applied to the study of the neural correlates of neuroticism. For instance, recent studies demonstrated that connectivity patterns in the amygdala and other structures involved in emotion regulation (including the prefrontal cortex) are modulated by different levels of neuroticism (Gao et al., 2013; Kruschwitz et al., 2014). ReHo in prefrontal cortex, particularly the middle frontal gyrus, was negatively modulated by neuroticism as well (Wei et al., 2011). Finally, Wei and coworkers showed a relationship between specific frequencies as measured by fALFF and neuroticism (Wei et al., 2014b). Specifically, they found a direct relationship in the right posterior portion of the frontal lobe, and an inverse one in the bilateral superior temporal cortex. Conversely, another study, using the entire spectrum of frequencies obtained through fALFF, demonstrated an inverse correlation between this metric and neuroticism in the precuneus and in the

middle frontal gyrus (Kunisato et al., 2011). These findings show that different methodologies identified significantly heterogeneous patterns of regional neural activity at rest.

Additional approaches can be used to assess the brain resting state activity, including global connectivity (GC), which measures the average connectivity between any given brain voxel and all the other brain voxels (Di et al., 2013), or measurements of complexity, such as the Hurst Exponent (HE) (Gentili et al., 2015; Hahn et al., 2012; Sokunbi et al., 2014). The HE provides a model of 1/f-like behaviors based on fractional Gaussian Noise (fGN) (Mandelbrot and Van Ness, 1968). In particular, a higher HE (closer to 1) defines a more predictable time series, while a lower HE (closer to 0.5) defines a less predictable, more chaotic time series.

While typically in brain activation studies the focus is on whether a certain area responds to a given task and to what extent its response changes across different conditions, in the study of the brain resting state neural activity the main issue is that different metrics may each capture just a portion of the resting state activity and consequently portray an incomplete and heterogeneous picture. Thus, identifying a region modulated by a given psychological trait is just a part of the issue, since results may vary depending on the metric utilized. For instance, functional connectivity describes the relationship among areas and consequently is thought to reflect interregional flows of information. However, functional connectivity provides no information on intrinsic, segregated neuronal activity (Lu and Stein, 2014; Raichle, 2015). On the contrary, LFO measures and REHO are more related to intrinsic local brain activity, although they concern distinct properties of the neural signal and thus provide different information. Finally, measures of complexity seem to be able to quantify the interplay between the first two types of metrics, to evaluate both segregated and integrated contributions to the regional activity (Jao et al., 2013).

We argue that this assortment of indices that provide only a fragmented description of the brain resting activity is an important reason for the lack of consistency across studies seeking to identify resting state correlates of psychological traits. We hold that a comprehensive evaluation of any psychological dimension cannot be pursued considering only one, or a few, metrics. To overcome these limitations, we designed a resting state fMRI experiment aiming to portray a multiparametric description of the neural correlates of neuroticism by using measurements of connectivity, REHO, complexity and LFO. Specifically, we seek to demonstrate within the same dataset that different metrics do indeed portray different aspects of the neurobiology of neuroticism and that the brain resting state neural activity as measured by fMRI is not only a matter of topography, but also of *functions* (i.e., of the characteristics of neuronal activity). Based on data from the above-mentioned literature on resting state modulation of neuroticism, we hypothesized that brain activity in regions related to the processing (e.g., superior temporal sulcus), expression (e.g., amygdala, insula, cingulate cortices) and regulation (e.g., inferior frontal gyrus, prefrontal cortex) of emotions would be modulated by neuroticism scores. Emotional regulation may affect several other mental functions, including reasoning and memory. (Forsman et al., 2012; Richards and Gross, 2000; Westen et al., 2006). Therefore, we hypothesized that different metrics would be modulated in different ways in key regions related to the processing and expression of emotion, and that this differential modulation may extend to regions related to other high-cortical functions as well.

2. Methods

2.1 Subjects

Thirty-one healthy volunteer participants were recruited for the present studies (25F/6M, mean age±s.d.: 25±3 years). All subjects were right-handed, drug-free and received a clinical examination to exclude history or presence of any medical, neurological, or psychiatric disorders that could affect brain function. None of the participants had first-degree relatives with history of psychiatric disorders as well. All participants gave their written informed consent to the study, which had been approved by the Ethical Committee at the Babes-Bolyai University, Cluj-Napoca, Romania.

2.2 Psychological measurements

To assess neuroticism we used the Anxiety-Neuroticism factor of the Romanian Version of Zuckerman Kuhlman Personality Questionnaire (ZKPQ), administered in the week prior to the fMRI scan. The ZKPQ (Zuckerman et al., 1993) represents a five-factor (Impulsive Sensation Seeking, Neuroticism-Anxiety, Aggression-Hostility, Sociability and Activity) personality inventory containing 99 true-false items. The Romanian adaptation of this scale presents an adequate internal consistency (α ranging from .69 to .88) and a good convergent validity (Sarbescu and Negut, 2013).

2.3 MRI data acquisition

A single Echo Planar Image of 512 time-points (15 minutes duration) was obtained in each fMRI session using a 3T Siemens Skyra Scanner (32 Channel Coil). The sequence had the following parameters 18 4-mm-thick axial slices (with 1-mm gap) (TR/TE = 1640/40ms, FA 90◦, FOV= 24 cm, resolution = 94×94 pixels). High-resolution anatomical brain scan was acquired with a T1-weighted spoiled gradient recall sequence (190 slices, 0.6-mm-thick sagittal images –voxel dimension 1*1 mm).

Subjects were all scanned after a full night of sleep and were instructed to lie in the scan with eyes closed and to relax without falling asleep. Upon completion of the resting state acquisition, we asked the subjects whether they felt asleep at any time during the fMRI sequence.

2.4 Data analysis

2.4.1 Common data preprocessing

We used the AFNI package (Cox, 1996) for spatial and time registration. Spatial registration was performed with the program *3dvolreg*. Time registration was used to compensate for slice acquisition delays and was obtained by using the program *3dTshift*. Residual movement related effects were first removed using a linear regression approach. In fact, signal changes related to head movements cannot be fully compensated by spatial realignment. These artifactual signals are generated by movement-dependent modulation of magnetization history of voxels (Friston et al., 1996). Six time-series describing three rigid body translations and three rigid body rotations of the head across time were obtained from the volume registration algorithm. These series were used in a multiple regression model at each voxel. Time dependent regressor was also included to linear detrended voxel time-series. Time-series that underwent further processing were consequently obtained as the residuals of the model.

2.4.2 HE calculation

After these pre-processing steps, we used fractional Gaussian noise (fGn) to describe the time series (Maxim et al., 2005). In particular, fGn can be modeled as a stochastic process, whose behavior can be characterized by its auto-covariance function. The fGn can be seen as the increment of a fractional Brownian motion sequence (fBm) sequence. This implies that a fBm sequence $B_{HE}(n)$ can be obtained as:

$$B_{HE}(n) = \sum_{k=0}^{n} G_{HE}(k) \qquad (1)$$

where $G_{HE}(k)$ are the samples of a fGn sequence. The equation (1) was used to obtain a fBm sequence from the movement corrected and linear detrended voxel time-series. The HE was estimated from this sequence by adopting the discrete second-order derivative approach (Istas and Lang, 1997; Kiviniemi et al., 2009) as implemented by the *wfbmesti* function of the Wavelet Toolbox of the Matlab package.

2.4.3 Preprocessing steps for the calculation of ALFF, fALFF, REHO and functional connectivity.

According to standard literature on resting state data processing, we performed further common steps for the above-mentioned analysis. Specifically, two time-series obtained from two spherical ROIs (4-mm radius) centered in the left lateral ventricle and in the corpus callosum were added to the multiple regression model described in 2.4.1 to control for white matter (WM) and cerebrospinal fluid (CSF) signals, respectively.

2.4.4 ALFF and fALFF calculation.

ALFF and fALFF parameters were estimated on a voxel-by-voxel basis from fMRI time-series as in Zang and colleagues (Zang et al., 2007) and in Zou and colleagues (Zou et al., 2008) respectively. In both cases, the parameters were estimated with the *3dRFSC* command of the AFNI package. For the ALFF calculation, this function estimates the power spectrum of each voxel's time series between 0.01 and 0.1 Hz, using the Fast Fourier Transform (FFT). Specifically, the signal was transformed in the frequency domain using FFT and the frequency bins within the frequency interval of interest were retained for the power spectrum computation. The ALFF was then estimated by taking the average between 0.01 and 0.1Hz of the square root of the power spectrum (Zang et al., 2007). As far as the fALFF parameter is concerned, the sum of the square root of the power spectrum components between

0.01 and 0.1 Hz was divided by the sum of the power spectrum components estimated across the entire frequency range (for the used TR, this interval corresponded to 0-0.30 Hz) (Zou et al., 2008).

2.4.5 Functional connectivity calculations.

As far as functional connectivity is concerned, we calculated two measurements: GC and ROI based maps for right and left amygdala connectivity. To estimate these metrics, motion outliers were detected by using the root mean square intensity difference (DVARS) (Power et al., 2012) of volume N to volume N+1. This was achieved using the program *fsl_motion_outliers* of the FSL distribution. Outliers were indentified as those values over the 75^{th} percentile +1.5 * Inter quartile range. The outliers were substituted with an interpolated value obtained using the program *3dTproject* of the AFNI distribution. Functional connectivity was estimated on the band filtered signal, (0.01 Hz < f < 0.10 Hz) to reduce the artifactual contribution due to physiological noise sources(Lowe et al., 1998). Bandpass filtering was achieved by using 3dTproject program.

GC was defined as the connectivity strength, i.e. the correlation coefficient, of each brain voxel with the mean time series derived from all the brain voxels. To perform such a calculation we used the program *3dTcorrMap* of the AFNI package. As ROI for the amygdalae we used the anatomical probabilistic ROI for the two amygdalae (probability threshold: 0.5) from the Cytoarchitectonic probabilistic atlas by Eickhoff and colleagues (Eickhoff et al., 2005), implemented in the AFNI distribution. The extracted time series were used as the input for correlation analysis through the program *3dfim+* of the AFNI package. Two different maps for each of the two amygdalae were obtained.

2.4.6. REHO calculation

REHO calculation was performed with the command 3dReHo of the FATCAT toolbox (Taylor and Saad, 2013). The neighborhood number of voxels was 27 to include face-, edge-, and node-wise neighbors. For the REHO analysis we performed the same movement outliers interpolation and the same bandpass filtering operation that were used for the estimation of functional connectivity measures.

2.4.7. Group analysis

To perform the group analysis, the maps of HE ALFF, fALFF, connectivity and REHO for each subject were re-sampled into standardized Talairach space ($1mm^3$ isovoxel volume) using a linear transformation (Talairach and Tournoux, 1988). We then performed a linear regression analysis (with the *3dttest++* command of AFNI package) on the whole brain where the score of neuroticism was used as the predictor to estimate each of the above-mentioned metric (criterion). We calculated the Family Wise Error (FWE) with a Montecarlo simulation through the *3dClustSim* command of the AFNI package. For this simulation, we estimated the mean full width half maximum (FWHM) of the spatial structure of the noise with the command *3dFWHMx* applied on a time series of residuals obtained from the command *3dDeconvolve* both of AFNI package. We performed this estimation both on unsmoothed (for HE calculation) and smoothed data. The simulation was performed on a mask (693,261 voxels) including only voxels of gray matter common to all subjects. According to these calculations, we considered significant those clusters with a size > 95 µl for a p value < 0.01 (corresponding to a FWE < 0.05). It is relevant to underline that the FWE calculation was performed with the emended version of 3dClustSim of the AFNI distribution. Such new version corrected a precedent bias. This version also has the option to consider the non guassianity of the noise distribution (Eklund et al., 2016). The effect

of non-gaussianity seems to be related to task design data analysis. However, we also considered the non gaussianity of the noise distribution in our simulations.

2.4.8 Metrics overlapping

As we indented to illustrate whether specific areas are more broadly modulated by Neuroticism – that is, independently from the metric taken into account –, the significant clusters from each maps ($p < 0.01$ corrected) were overlapped as binary masks. In the resulting overlapped map, we considered significant only those clusters that resulted from the overlapping of at least three different metrics and above the size of 95 μl, as defined before. For this reason, each metric may contribute to clusters in the overlapped maps although the same clusters do not reach the statistical volume-threshold in the single metric analysis.

3. Results

3.1 Psychological and behavioral results

Neuroticism score was 6.8 ± 4.2 (mean ± s.d.), ranging between 1 and 14 (maximum score 19). Grubb's test for outliers did not find any outlier in the score distribution. None of the subjects reported to have fallen asleep during the resting state acquisition.

3.2 fMRI results

All the metrics correlated with neuroticism in different brain areas (see tables 1 and 2 and figures 1-3). In particular, the brain regions that were significantly modulated by neuroticism scores were: Posterior Cingulate and precuneus (PCC/precun), Anterior Cingualte (ACC), Medial Frontal Gyrus (MFG), Inferior Parietal Lobule (IPL) for ALFF; Inferior Frontal Gyrus (IFG), thalamus, fusiform gyrus, Superior Frontal Gyrus (SFG), IFG, SFG, cingulate gyrus, Middle Frontal Gyrus (MidFG), Superior Parietal Lobule (SPL), IPL and cuneus for fALFF; amygdala, precuneus, SFG, MidFG, fusiform gyrus, MFG, IFG, Middle Temporal Gyrus (MidTG), Superior Temporal Sulcus (STS), ACC, precentral gyrus (preCG) for REHO; IPL, amygdala, precuneus, IFG, parahippocampal gyrus, MidTG, Transverse Temporal Gyrus (TTG), OrbitoFrontal Gyrus (OFG), STS, thalamus, ACC for Hurst Exponent; amygdala, IFG, lingual gyrus, MidFG for Global Connectivity; Supramarginal gyrus (SMG), Inferior Occipital Gyrus (IOG), cuneus, fusiform gyrus, preCG, IFG, temporal pole, amygdala, insula, SMG, STS, lingual gyrus, Superior Occipital Gyrus (SOG), IPL, middle Occipital Gyrus (midOG), SPL, postCG, Medial Temporal Gyrus (MTG), for left amygdala connectivity; angular gyrus, MTG, amygdala, cingulate cortex, Medial Occipital Gyrus (MOG), Medial orbital Gyrus, MTG, hippocampus, IFGm precuneus, insula, MTG, SMG.

We did not find a complete dissociation among metrics, since neuroticism scores modulated multiple metrics within the same areas. However, the overlapping map did not find any regions in

which all the metrics were influenced by neuroticism levels at the same time; just in two clusters (IFG and right amygdala) four out of the seven measures were significantly modulated by the degree of neuroticism (table 3 and figure 4). As far as the metrics that were more present in the common clusters are concerned, REHO contributed to four out of five significant clusters, while the fALFF only to three. The HE was the metric that contributed the less to the common clusters, being present in only one cluster.

4. Discussion

Psychological traits are stable aspects of mindset and, as such, should arguably be reflected by stable configurations in brain activity, detectable even when the individual is not engaged in any specific activity. Given the complexity typically encapsulated in psychological traits and the vast amount of information present in the resting state signal, we sustain that studying the neurobiology of personality by relying on just one type of index is overly reductionist and bound to provide a fragmented picture. Consequently, we used multiple metrics to evaluate the modulatory effects of neuroticism on resting state brain activity.

4.1. LFO metrics (ALFF-fALFF)

LFO metrics are considered a measure of components of the BOLD signal, intrinsically related to the neurovascular coupling (Jao et al., 2013; Zang et al., 2007; Zou et al., 2008). In our study, we found that neuroticism modulated ALFF in the precuneus, prefrontal cortex, and inferior parietal lobule, while fALFF was modulated by neuroticism in precuneus, prefrontal cortex and visual cortex.

Specifically, regions related to emotional regulation, like the prefrontal cortex, showed altered LFO with the increase in neuroticism: we found decreased LFO in IFG and an increased LFO in the other prefrontal regions (SFG, MFG, midFG). Alterations in structure and functional activity within the IFG in individuals with higher neuroticism were also reported by other studies and may represent the neural correlate of the reduced ability for the cognitive regulation of emotions (Bjørnebekk et al., 2013; Lu et al., 2014; Sosic-Vasic et al., 2012). Other studies have found alterations in connectivity and brain activity in MFG, midFG and, more generally, in the prefrontal cortex (Forbes et al., 2014; Szameitat et al., 2016; Tzschoppe et al., 2014). Alterations of the LFO metrics were also found in the DMN network confirming the relative vast literature linking DMN alterations to neuroticism (Sampaio et al., 2014; Wei et al., 2011; Wei et al., 2016). In particular, fALFF in the IPL and precuneus was reduced along

with the increase in neuroticism. It is interesting to note that in another cluster within the PCC/precuneus area, both ALFF and fALFF increased with higher levels of neuroticism. Conversely, ALFF showed an opposite pattern in the IPL, since it increased with the rise in neuroticism. The same direct linear relationship was present in the ACC. The significant clusters for fALFF and ALFF did not overlap. Therefore, we conclude that the two LFO metrics portray different modulation of neuroticism across distinct brain areas, consequently providing complementary information.

Two previous studies evaluated fALFF and its relationship with neuroticism. The results from our study are in line with the findings by Kunisato and colleagues who demonstrated an inverse correlation between fALFF and neuroticism in the precuneus and in the middle frontal cortex (Kunisato et al., 2011). However, we also found clusters in these regions in which fALFF increased with higher neuroticism. This result is partially in line with the findings obtained by Wei and coworkers (2011) showing a relationship between fALFF and neuroticism in the frontal cortex and in the superior termporal gyrus (Wei et al., 2011).

4.2 REHO

We found an inverse association between neuroticism and REHO in areas involved in emotional response (cingulate, amygdala), emotional regulation (inferior frontal) and mentalizing (STS), in, which REHO decreased with the increase in neuroticism. Our results partially overlap with those of Wei and colleagues (Wei et al., 2011), who also reported an inverse relationship between neuroticism and REHO in the inferior frontal cortex. However, we found positive correlation between REHO and neuroticism in the prefrontal cortex (SFG, MFG, MidFG), in the fusiform gyrus and in precuneus. As mentioned, the prefrontal cortex and DMN areas including the precuneus were found to be modulated by neuroticism both in resting state analysis, as well as during task (Forbes et al., 2014; Sampaio et al.,

2014; Szameitat et al., 2016; Tzschoppe et al., 2014; Wei et al., 2011; Wei et al., 2016). As far as the fusiform gyrus is concerned, Kruschwitz and colleagues showed an altered amygdala-fusiform gyrus connectivity in individuals with higher neuroticism (Kruschwitz et al., 2014). Nevertheless, they found this relationship within the right fusiform gyrus while, to our knowledge, our result is the first report of neuroticism modulation of brain activity in the left fusiform gyrus.

On the whole, these results are consistent with those for the LFO metrics. Moreover, both LFO metrics and REHO portray specific aspects of the brain local resting activity. An increased local coherence, indexed by the REHO, has been linked to the coordinated neuronal discharge typical of a task-related activation. Consequently, variations in REHO may represent an index of the potential to respond with an organized and coherent neuronal discharge (Zang et al., 2004). However, other authors have suggested that, although local, REHO may reflect in short-range brain dynamics properties of long-range whole-brain networks (Liang et al., 2013).

4.3 Hurst Exponent

None of previous studies on neuroticism measured HE. In the present study, HE was inversely correlated to neuroticism in regions related to emotional response (e.g., amygdala) and emotional regulation (e.g., inferior frontal gyrus). We also found significant clusters within the DMN (precuneus and inferior parietal gyrus), and theory of mind regions (STS, and MidTG). These results are similar to those reported with LFO metrics, suggesting that these measurements reflected similar, though not identical, processes.

However, HE also was the only metric that inversely correlated with neuroticism in the parahippocampal gyrus. The parahippocampal gyrus plays a pivotal role in the limbic system and appears to be a hub station for the connections between the amygdala and hippocampus (Stefanacci et al., 1996). The interplay of these structures was postulated to play a key role in the regulation of stress

(Ulrich-Lai and Herman, 2009) and in emotional learning (LaBar and Cabeza, 2006). Recently, parahippocampal volume was found to moderate the relationship between neuroticism and psychosomatic symptoms (Wei et al., 2014a), a relationship very well-known at the clinical level (Costa and McCrae, 1987; Netter and Hennig, 1998; Tanum and Malt, 2001). Specifically, neuroticism predicted psychosomatic complaints in the presence of a higher parahippocampal volume.

The HE is considered an index that takes into account both the intrinsic and extrinsic contributions to the BOLD-signal time-course. Namely, as it gives a compact measure of the predictability of a time series, the contributions of both the intrinsic regional discharge and the influence from the distant connected regions are allegedly taken into account (Jao et al., 2013).

The increase of chaoticity, or randomness/unpredictibility in these structures, which was associated with higher neuroticism, may be related to an alteration in spontaneous periodic discharge in emotional and cognitive brain structures. This purported lack of regulation may trigger an abnormal response while the individual copes with emotionally relevant situations. Conversely, HE positively correlated with neuroticism in both the precunues/posterior cingulate and in the anterior cingulate. Higher HE in the precuneus/posterior cingulate may be related to an increased rigidity of neural activity in this region. Like for fALFF, this may represent the neurobiological counterpart of increased rumination and self-focused attention, typical cognitive components in anxiety and neuroticism.

4.4 Amygdalae functional connectivity

We found that increased neuroticism scores were related to a wide modulation of the strength of connectivity between the two amygdalae and the visual cortical areas. In some of the clusters within the visual cortex, the connectivity positively correlated with neuroticism (e.g. MOG and lingual gyrus) while in others there was a negative correlation (e.g. cuneus). We also found a positive correlation between the fusiform gyrus and left amygdala. Our findings are partially consistent with those from the

only study on resting state functional connectivity, that reported a direct correlation between neuroticism and connectivity strength between the amygdalae and fusiform cortex bilaterally (Kruschwitz et al., 2014).

Additionally, we found a reduction in the connectivity strength between the right amygdalae and cingulate cortex, which is consistent with the findings obtained by Cremer and colleagues during a face perception task (Cremers et al., 2010). In line with them, we speculate that such a decrement was related to the loosening of the control of the cingulate cortex over the discharge of the amygdala. More in general, our resting state data showed that with the augment in neuroticism scores, the connectivity of the bilateral amygdala with a range of areas decreased. These areas were related not only to emotions (insula, ACC and precuneus), but also to cognition, memory and perception (STS, hippocampus and prefrontal cortex). Notably, this modulation was present in the connectivity between the left and right amygdala as well. We hypothesized that the loss of synchronicity between the two amygdalae may be due to the increased chaotic pattern of discharge of these regions. Such an augment in chaos is coherent with the results obtained with the HE.

4.5.Global connectivity

To our knowledge, the present study is the first to evaluate the relationship between global connectivity and personality traits. Of note, in our data, global connectivity was decreased in emotional regulation structures (like amgydala, IFG and MidFG) and in visual areas (lingual gyrus). In this sense, we suggest that global disconnection of these structures may be related to the difficulties in emotional regulation and hyperactivity, which are typical in highly neurotic subjects. Particularly, we would argue that the functional connectivity breakdown may impair the integration of information. Since this breakdown was localized in emotional regulation regions as well as in the visual cortex, we suggest

that neuroticism may affect the wide-ranging network fundamental for dealing with emotions in an efficient way.

Only a few studies to date have evaluated this measure and the way in which it can be affected by psychological dimensions and by psychopathology. For instance, Cole and colleagues found that intelligence correlated with global connectivity in the prefrontal cortex (Cole et al., 2012), while alterations of global connectivity were related to obsessive-compulsive disorder (Anticevic et al., 2014). Finally, an altered global connectivity was seen in ketamine-assuming subjects who showed schizophrenic-like symptoms (Driesen et al., 2013).

4.6 Limitations

A potential limitation of the present study is the lack of control for heart rate and respiration, as we did not monitor these signals. In particular, functional connectivity seems to be highly affected by heart rate and respiration with the risk of introducing false positives (Jo et al., 2010; Khalili-Mahani et al., 2013). However, other metrics, like fALFF and HE, appear to be much less affected by physiological noise (Jao et al., 2013; Zou et al., 2008). Furthermore, we regressed out white matter and cerebrospinal fluid signals, though we cannot rule out completely the possibility that our results were influenced by residual confounds related to physiological signal changes.

Another potential limitation of our study is related to the individual sample. Although both individuals with very low and high scores in neuroticism were included, the study did not cover the entire range of the scale. Future studies with larger groups of subjects, including also patients with anxiety and mood disorders, who typically show very high levels of neuroticism, may contribute to clarify if the present findings extend to the entire range of the trait.

Finally, regarding the overlapping map, it is necessary to underline that it mainly has an illustrative purpose to show the regions that are more often modulated by neuroticism. Importantly,

each of the clusters contributing to this map was FEW corrected and we reported only the clusters over the FWE cluster correction size (>95 microliters). Notably, FWE correction implies that at least one of the voxel in the clusters over the threshold is not a false positive detection. However, it is not possible to ascertain which voxels among those that result significantly activated are not false positive ones. In turn, this implies that we cannot determine to what extent the voxels that overlap are those that are truly significantly activated and not false positives

4.7. Conclusions

To our knowledge this is the first study to demonstrate the importance of a multiparametric approach to the brain resting state fMRI data in the study of the neurobiological underpinnings of psychological traits. Given that different metrics portray different aspects of the resting state signal, a multiparametric approach is necessary to achieve a more complete picture of the psychological trait being studied. We claim that this approach should be considered both for basic research on psychological and psychopathological traits as well as when neuroimaging methods are applied to clinical or forensic matters (Rigoni et al., 2010; Sartori et al., 2011).

When projecting the results of the different metrics on a single map, a partial overlap among regions was detected. In particular, the different metrics were consistently modulated by neuroticism in regions related to emotion regulation, including the inferior frontal, middle frontal and precentral cortex, to emotional reactivity, such as the amygdala, to self-evaluation and introspection, like the precuneus. These results confirm our exploratory hypothesis that different metrics often convey largely different and not redundant information. Hence, all the metrics should be analyzed when studying the neurobiological correlates of psychological or psychopathological processes by measuring brain resting state activity. In our work, some metrics seemed to be less informative or specific, while others, for instance REHO and LFO, modulated similar clusters. Therefore, arguing that all the metrics considered

should hold the same weight when studying the impact of psychological traits on resting state may be a bit too strong conclusion. However, we would maintain that in the context of an exploratory study, a wide multi-metric approach should be considered in order to pinpoint the more informative measure of brain activity. In this sense, different metrics portray different aspects of the modulatory effect of personality traits on brain dynamics. Conversely, focusing only on one metric, may give an incomplete and hence misleading description of the psychological traits.

Acknowledgments

Ioana A. Cristea was financially supported by a Young Researcher Grant (GTC_34064/2013), awarded by the Babes-Bolyai University, Romania and by a Visiting Research Grant from the University of Padua (granted to Claudio Gentili).

This study was partially supported by Fondazione IRIS – Castagneto Carducci, Livorno, Italy.

The Authors declare no conflict of interests.

References

Anticevic, A., Hu, S., Zhang, S., Savic, A., Billingslea, E., Wasylink, S., Repovs, G., Cole, M.W., Bednarski, S., Krystal, J.H., Bloch, M.H., Li, C.S., Pittenger, C., 2014. Global resting-state functional magnetic resonance imaging analysis identifies frontal cortex, striatal, and cerebellar dysconnectivity in obsessive-compulsive disorder. Biol Psychiatry 75, 595-605.

Barkhof, F., Haller, S., Rombouts, S.A., 2014. Resting-state functional MR imaging: a new window to the brain. Radiology 272, 29-49.

Bjørnebekk, A., Fjell, A.M., Walhovd, K.B., Grydeland, H., Torgersen, S., Westlye, L.T., 2013. Neuronal correlates of the five factor model (FFM) of human personality: Multimodal imaging in a large healthy sample. Neuroimage 65, 194-208.

Cole, M.W., Yarkoni, T., Repovs, G., Anticevic, A., Braver, T.S., 2012. Global connectivity of prefrontal cortex predicts cognitive control and intelligence. J Neurosci 32, 8988-8999.

Costa, P.T., McCrae, R.R., 1987. Neuroticism, somatic complaints, and disease: is the bark worse than the bite? J Pers 55, 299-316.

Cox, R.W., 1996. AFNI: software for analysis and visualization of functional magnetic resonance neuroimages. Computers and Biomedical Research, an International Journal 29, 162-173.

Cremers, H.R., Demenescu, L.R., Aleman, A., Renken, R., van Tol, M.J., van der Wee, N.J., Veltman, D.J., Roelofs, K., 2010. Neuroticism modulates amygdala-prefrontal connectivity in response to negative emotional facial expressions. Neuroimage 49, 963-970.

Daffern, M., Gilbert, F., Lee, S., Chu, C.M., 2015. The relationship between early maladaptive schema, psychopathic traits, and neuroticism in an offender sample. Clinical Psychologist.

Damoiseaux, J.S., Rombouts, S.A.R.B., Barkhof, F., Scheltens, P., Stam, C.J., Smith, S.M., Beckmann, C.F., 2006. Consistent resting-state networks across healthy subjects. Proceedings of the National Academy of Sciences of the United States of America 103, 13848-13853.

Deco, G., Jirsa, V.K., McIntosh, A.R., 2011. Emerging concepts for the dynamical organization of resting-state activity in the brain. Nature Reviews. Neuroscience 12, 43-56.

Derryberry, D., Reed, M.A., 1994. Temperament and attention: orienting toward and away from positive and negative signals. J Pers Soc Psychol 66, 1128-1139.

Di, X., Gohel, S., Kim, E.H., Biswal, B.B., 2013. Task vs. rest-different network configurations between the coactivation and the resting-state brain networks. Frontiers in human neuroscience 7, 493.

Driesen, N.R., McCarthy, G., Bhagwagar, Z., Bloch, M., Calhoun, V., D'Souza, D.C., Gueorguieva, R., He, G., Ramachandran, R., Suckow, R.F., Anticevic, A., Morgan, P.T., Krystal, J.H., 2013. Relationship of resting brain hyperconnectivity and schizophrenia-like symptoms produced by the NMDA receptor antagonist ketamine in humans. Mol Psychiatry 18, 1199-1204.

Eklund, A., Nichols, T.E., Knutsson, H., 2016. Cluster failure: Why fMRI inferences for spatial extent have inflated false-positive rates. Proceedings of the National Academy of Sciences of the United States of America 113, 7900-7905.

Forbes, C.E., Poore, J.C., Krueger, F., Barbey, A.K., Solomon, J., Grafman, J., 2014. The role of executive function and the dorsolateral prefrontal cortex in the expression of neuroticism and conscientiousness. Soc Neurosci 9, 139-151.

Forsman, L.J., de Manzano, O., Karabanov, A., Madison, G., Ullen, F., 2012. Differences in regional brain volume related to the extraversion-introversion dimension--a voxel based morphometry study. Neurosci Res 72, 59-67.
Friston, K.J., Williams, S., Howard, R., Frackowiak, R.S., Turner, R., 1996. Movement-related effects in fMRI time-series. Magnetic resonance in medicine: official journal of the Society of Magnetic Resonance in Medicine / Society of Magnetic Resonance in Medicine 35, 346-355.
Gao, Q., Xu, Q., Duan, X., Liao, W., Ding, J., Zhang, Z., Li, Y., Lu, G., Chen, H., 2013. Extraversion and neuroticism relate to topological properties of resting-state brain networks. Front Hum Neurosci 7, 257.
Gentili, C., Vanello, N., Cristea, I., David, D., Ricciardi, E., Pietrini, P., 2015. Proneness to social anxiety modulates neural complexity in the absence of exposure: A resting state fMRI study using Hurst exponent. Psychiatry Res 232, 135-144.
Hahn, T., Dresler, T., Ehlis, A.-C., Pyka, M., Dieler, A.C., Saathoff, C., Jakob, P.M., Lesch, K.-P., Fallgatter, A.J., 2012. Randomness of resting-state brain oscillations encodes Gray's personality trait. NeuroImage 59, 1842-1845.
Istas, J., Lang, G., 1997. Quadratic variations and estimation of the local Hölder index of a Gaussian process. Annales de l'institut Henri Poincare (B) Probability and Statistics 33, 407-436.
Jao, T., Vertes, P.E., Alexander-Bloch, A.F., Tang, I.N., Yu, Y.C., Chen, J.H., Bullmore, E.T., 2013. Volitional eyes opening perturbs brain dynamics and functional connectivity regardless of light input. Neuroimage 69, 21-34.
Jo, H.J., Saad, Z.S., Simmons, W.K., Milbury, L.A., Cox, R.W., 2010. Mapping sources of correlation in resting state FMRI, with artifact detection and removal. NeuroImage 52, 571-582.
Kendler, K.S., Gatz, M., Gardner, C.O., Pedersen, N.L., 2006. Personality and major depression: a Swedish longitudinal, population-based twin study. Arch Gen Psychiatry 63, 1113-1120.
Kendler, K.S., Kuhn, J., Prescott, C.A., 2004. The interrelationship of neuroticism, sex, and stressful life events in the prediction of episodes of major depression. Am J Psychiatry 161, 631-636.
Khalili-Mahani, N., Chang, C., van Osch, M.J., Veer, I.M., van Buchem, M.A., Dahan, A., Beckmann, C.F., van Gerven, J.M.A., Rombouts, S.A.R.B., 2013. The impact of "physiological correction" on functional connectivity analysis of pharmacological resting state fMRI. NeuroImage 65, 499-510.
Kiviniemi, V., Remes, J., Starck, T., Nikkinen, J., Haapea, M., Silven, O., Tervonen, O., 2009. Mapping Transient Hyperventilation Induced Alterations with Estimates of the Multi-Scale Dynamics of BOLD Signal. Frontiers in neuroinformatics 3, 18.
Kotov, R., Gamez, W., Schmidt, F., Watson, D., 2010. Linking "big" personality traits to anxiety, depressive, and substance use disorders: a meta-analysis. Psychol Bull 136, 768-821.
Kruschwitz, J.D., Walter, M., Varikuti, D., Jensen, J., Plichta, M.M., Haddad, L., Grimm, O., Mohnke, S., Pöhland, L., Schott, B., Wold, A., Mühleisen, T.W., Heinz, A., Erk, S., Romanczuk-Seiferth, N., Witt, S.H., Nöthen, M.M., Rietschel, M., Meyer-Lindenberg, A., Walter, H., 2014. 5-HTTLPR/rs25531 polymorphism and neuroticism are linked by resting state functional connectivity of amygdala and fusiform gyrus. Brain Struct Funct.
Kunisato, Y., Okamoto, Y., Okada, G., Aoyama, S., Nishiyama, Y., Onoda, K., Yamawaki, S., 2011. Personality traits and the amplitude of spontaneous low-frequency oscillations during resting state. Neurosci Lett 492, 109-113.
LaBar, K.S., Cabeza, R., 2006. Cognitive neuroscience of emotional memory. Nat Rev Neurosci 7, 54-64.
Liang, M.-J., Zhou, Q., Yang, K.-R., Yang, X.-L., Fang, J., Chen, W.-L., Huang, Z., 2013. Identify changes of brain regional homogeneity in bipolar disorder and unipolar depression using resting-state FMRI. PLoS One 8, e79999.

Lowe, M.J., Mock, B.J., Sorenson, J.A., 1998. Functional connectivity in single and multislice echoplanar imaging using resting-state fluctuations. Neuroimage 7, 119-132.
Lu, F., Huo, Y., Li, M., Chen, H., Liu, F., Wang, Y., Long, Z., Duan, X., Zhang, J., Zeng, L., Chen, H., 2014. Relationship between personality and gray matter volume in healthy young adults: a voxel-based morphometric study. PLoS One 9, e88763.
Lu, H., Stein, E.A., 2014. Resting state functional connectivity: its physiological basis and application in neuropharmacology. Neuropharmacology 84, 79-89.
Mandelbrot, B.B., Van Ness, J.W., 1968. Fractional Brownian Motions, Fractional Noises and Applications. SIAM Review 10, 422-437.
Maxim, V., Sendur, L., Fadili, J., Suckling, J., Gould, R., Howard, R., Bullmore, E., 2005. Fractional Gaussian noise, functional MRI and Alzheimer's disease. NeuroImage 25, 141-158.
Netter, P., Hennig, J., 1998. The fibromyalgia syndrome as a manifestation of neuroticism? Z Rheumatol 57 Suppl 2, 105-108.
Pannekoek, J.N., Veer, I.M., van Tol, M.-J., van der Werff, S.J.A., Demenescu, L.R., Aleman, A., Veltman, D.J., Zitman, F.G., Rombouts, S.A.R.B., van der Wee, N.J.A., 2013. Resting-state functional connectivity abnormalities in limbic and salience networks in social anxiety disorder without comorbidity. European neuropsychopharmacology: the journal of the European College of Neuropsychopharmacology 23, 186-195.
Peterson, A., Thome, J., Frewen, P., Lanius, R.A., 2014. Resting-state neuroimaging studies: a new way of identifying differences and similarities among the anxiety disorders? Can J Psychiatry 59, 294-300.
Power, J.D., Barnes, K.A., Snyder, A.Z., Schlaggar, B.L., Petersen, S.E., 2012. Spurious but systematic correlations in functional connectivity MRI networks arise from subject motion. Neuroimage 59, 2142-2154.
Raichle, M.E., 2015. The restless brain: how intrinsic activity organizes brain function. Philos Trans R Soc Lond B Biol Sci 370.
Richards, J.M., Gross, J.J., 2000. Emotion regulation and memory: the cognitive costs of keeping one's cool. J Pers Soc Psychol 79, 410-424.
Rigoni, D., Pellegrini, S., Mariotti, V., Cozza, A., Mechelli, A., Ferrara, S.D., Pietrini, P., Sartori, G., 2010. How neuroscience and behavioral genetics improve psychiatric assessment: report on a violent murder case. Front Behav Neurosci 4, 160.
Sampaio, A., Soares, J.M., Coutinho, J., Sousa, N., Gonçalves, Ó.F., 2014. The Big Five default brain: functional evidence. Brain Struct Funct 219, 1913-1922.
Sarbescu, P., Negut, A., 2013. Psychometric Properties of the Romanian Version of the Zuckerman-Kuhlman Personality Questionnaire. European Journal of Psychological Assessment 29, 241-252.
Sartori, G., Pellegrini, S., Mechelli, A., 2011. Forensic neurosciences: from basic research to applications and pitfalls. Current opinion in neurology 24, 371-377.
Servaas, M.N., Riese, H., Renken, R.J., Marsman, J.B., Lambregs, J., Ormel, J., Aleman, A., 2013. The effect of criticism on functional brain connectivity and associations with neuroticism. PLoS One 8, e69606.
Sokunbi, M.O., Gradin, V.B., Waiter, G.D., Cameron, G.G., Ahearn, T.S., Murray, A.D., Steele, D.J., Staff, R.T., 2014. Nonlinear complexity analysis of brain FMRI signals in schizophrenia. PLoS One 9, e95146.
Sosic-Vasic, Z., Ulrich, M., Ruchsow, M., Vasic, N., Grön, G., 2012. The modulating effect of personality traits on neural error monitoring: evidence from event-related FMRI. PLoS One 7, e42930.

Stefanacci, L., Suzuki, W.A., Amaral, D.G., 1996. Organization of connections between the amygdaloid complex and the perirhinal and parahippocampal cortices in macaque monkeys. J Comp Neurol 375, 552-582.
Szameitat, A.J., Saylik, R., Parton, A., 2016. Neuroticism related differences in the functional neuroanatomical correlates of multitasking. An fMRI study. Neurosci Lett 635, 51-55.
Talairach, J., Tournoux, P., 1988. Co-planar stereotaxic atlas of the human brain : 3-dimensional proportional system : an approach to cerebral imaging. Thieme, Stuttgart.
Tanum, L., Malt, U.F., 2001. Personality and physical symptoms in nonpsychiatric patients with functional gastrointestinal disorder. J Psychosom Res 50, 139-146.
Taylor, P.A., Saad, Z.S., 2013. FATCAT: (an efficient) Functional and Tractographic Connectivity Analysis Toolbox. Brain Connect 3, 523-535.
Tzschoppe, J., Nees, F., Banaschewski, T., Barker, G.J., Büchel, C., Conrod, P.J., Garavan, H., Heinz, A., Loth, E., Mann, K., Martinot, J.-L., Smolka, M.N., Gallinat, J., Ströhle, A., Struve, M., Rietschel, M., Schumann, G., Flor, H., consortium, I., 2014. Aversive learning in adolescents: modulation by amygdala-prefrontal and amygdala-hippocampal connectivity and neuroticism. Neuropsychopharmacology 39, 875-884.
Ulrich-Lai, Y.M., Herman, J.P., 2009. Neural regulation of endocrine and autonomic stress responses. Nat Rev Neurosci 10, 397-409.
Wei, D., Du, X., Li, W., Chen, Q., Li, H., Hao, X., Zhang, L., Hitchman, G., Zhang, Q., Qiu, J., 2014a. Regional gray matter volume and anxiety-related traits interact to predict somatic complaints in a non-clinical sample. Soc Cogn Affect Neurosci.
Wei, L., Duan, X., Yang, Y., Liao, W., Gao, Q., Ding, J.-r., Zhang, Z., Zeng, W., Li, Y., Lu, G., Chen, H., 2011. The synchronization of spontaneous BOLD activity predicts extraversion and neuroticism. Brain Res 1419, 68-75.
Wei, L., Duan, X., Zheng, C., Wang, S., Gao, Q., Zhang, Z., Lu, G., Chen, H., 2014b. Specific frequency bands of amplitude low-frequency oscillation encodes personality. Hum Brain Mapp 35, 331-339.
Wei, S., Su, Q., Jiang, M., Liu, F., Yao, D., Dai, Y., Long, L., Song, Y., Yu, M., Zhang, Z., Zhao, J., Guo, W., 2016. Abnormal default-mode network homogeneity and its correlations with personality in drug-naive somatization disorder at rest. J Affect Disord 193, 81-88.
Weinstock, L.M., Whisman, M.A., 2006. Neuroticism as a common feature of the depressive and anxiety disorders: a test of the revised integrative hierarchical model in a national sample. J Abnorm Psychol 115, 68-74.
Westen, D., Blagov, P.S., Harenski, K., Kilts, C., Hamann, S., 2006. Neural bases of motivated reasoning: an FMRI study of emotional constraints on partisan political judgment in the 2004 U.S. Presidential election. J Cogn Neurosci 18, 1947-1958.
Zang, Y., Jiang, T., Lu, Y., He, Y., Tian, L., 2004. Regional homogeneity approach to fMRI data analysis. Neuroimage 22, 394-400.
Zang, Y.-F., He, Y., Zhu, C.-Z., Cao, Q.-J., Sui, M.-Q., Liang, M., Tian, L.-X., Jiang, T.-Z., Wang, Y.-F., 2007. Altered baseline brain activity in children with ADHD revealed by resting-state functional MRI. Brain Dev 29, 83-91.
Zou, Q.H., Zhu, C.Z., Yang, Y., Zuo, X.N., Long, X.Y., Cao, Q.J., Wang, Y.F., Zang, Y.F., 2008. An improved approach to detection of amplitude of low-frequency fluctuation (ALFF) for resting-state fMRI: Fractional ALFF. Journal of Neuroscience Methods 172, -141.
Zuckerman, M., 2005. Psychobiology of personality, 2nd ed., rev. and updated ed. Cambridge University Press, Cambridge.

Zuckerman, M., Joireman, J., Kraft, M., Kuhlman, D.M., 1999. Where do motivational and emotional traits fit within three factor models of personality? Personality and Individual Differences 26, 487-504.
Zuckerman, M., Michael, D., Joireman, J., Teta, P., Kraft, M., 1993. A comparison of three structural models for personality: The Big Three, the Big Five, and the Alternative Five. Journal of Personality and Social Psychology 65, 757-768.

Figure and table legend:

Figure 1

Regions in which fALFF and ALFF metrics were modulated by neuroticism. Warm colors portrait positive correlations while cold ones portrait negative correlations ($p < 0.01$ FWE corrected).

Figure 2

Regions in which HE and REHO metrics were modulated by neuroticism. Warm colors portrait positive correlations while cold ones portrait negative correlations ($p < 0.01$ FWE corrected).

Figure 3

Regions in which functional global connectivity and functional connectivity, using left and right amygdalae as ROI, were modulated by neuroticism. Warm colors portrait positive correlations while cold ones portrait negative correlations ($p < 0.01$ FWE corrected).

Figure 4

Conjunction analysis for the metrics used in the study. Significant clusters for each metrics ($p < 0.01$) entered in the conjunction analysis. Cluster size correction (FWE) was performed on the conjunct map (cluster size > 280 μl for a FEW $p < 0.05$). red= 6 overlapping metrics; blue= 5 overlapping metrics; green = 4 overlapping metrics; yellow = 3 overlapping metrics

Table 1

Significant clusters in which fALFF, ALFF, REHO and HE metrics were modulated by neuroticism (all clusters $p < 0.01$, FWE corrected).

PCC/precun; posterior cingulate/ precuneus; IFG: inferior frontal gyrus; PreCG: Precentral Gyrus; IPL: inferior parietal lobule; STS: superior temporal sulcus; paraHip: parahippocampal gyrus; midTG: middle temporal gyrus; TTG: transversal temporal gyrus; OFG: orbitofrontal gyrus; ACC: anterior cingulate cortex

Table 2

Significant clusters in which GC and left and right amygdalae functional connectivity were modulated by neuroticism (all clusters $p < 0.01$, FEW corrected). PreCG: precentral gyrus; IFG: inferior frontal gyrus; STS: superior temporal sulcus; IPL: inferior parietal lobule; SFG: superior frontal gyrus; Fgyr: fusiform gyrus; SFG: superior frontal gyrus; STS: superior temporal sulcus; MedFG: medial frontal gyrus; IPL: inferior parietal lobule; postCG: postcentral gyrus; midFG: middle frontal gyrus; PCC: posterior cingulate cortex; Pcun: precuneus.

Table 3

Conjunction analysis for regions in which at least two metrics were modulated by neuroticism scores (aggregated clusters $p < 0.01$, FEW corrected). PreCG: precentral gyrus; IFG: inferior frontal gyrus; precun: precuneus; SFG: superior frontal gyrus; IFG: inferior frontal gyrus; STS: superior temporal sulcus.

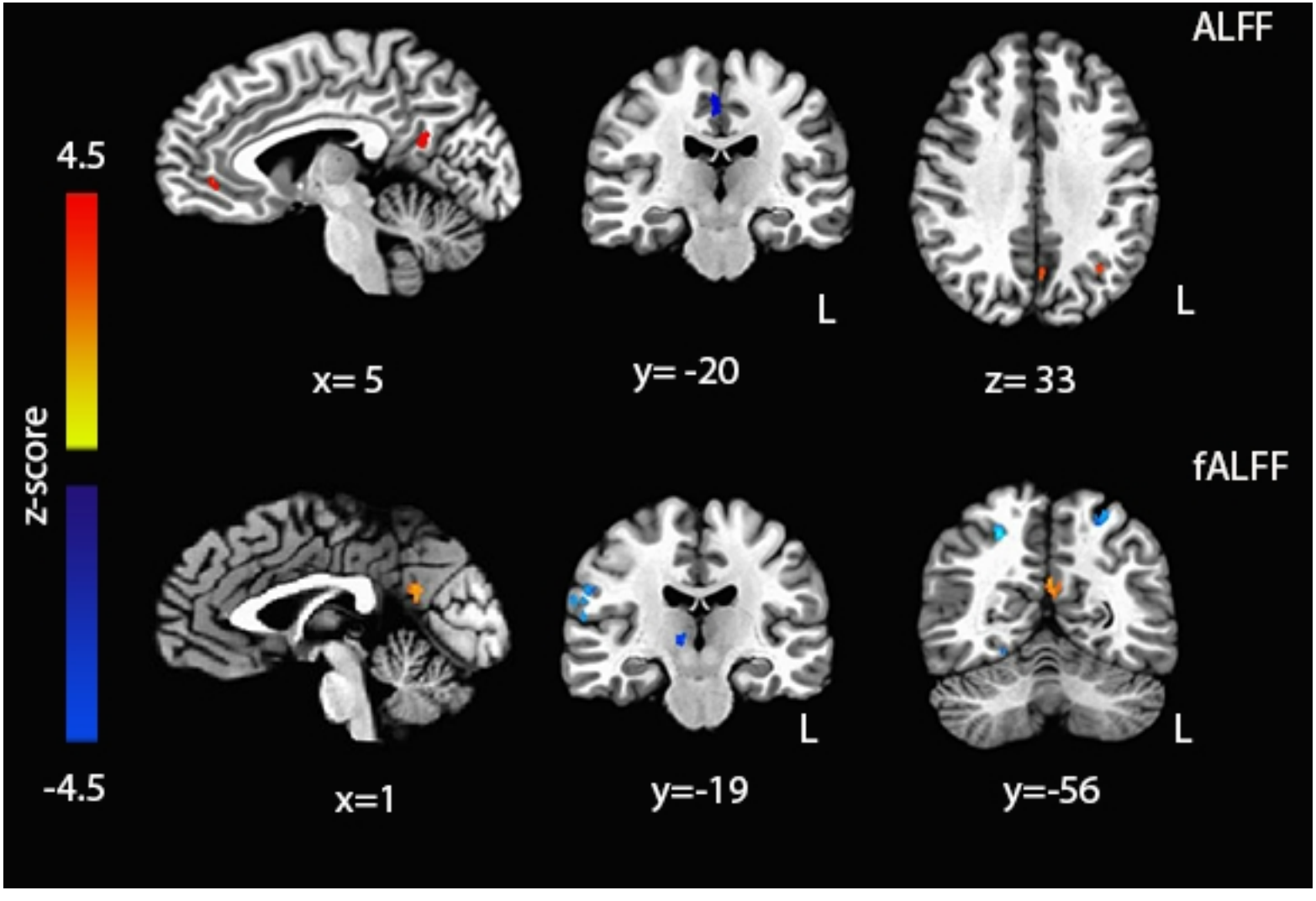
ALFF
4.5
z-score
-4.5
x= 5
y= -20
z= 33
L
L
fALFF
x=1
y=-19
y=-56
L
L

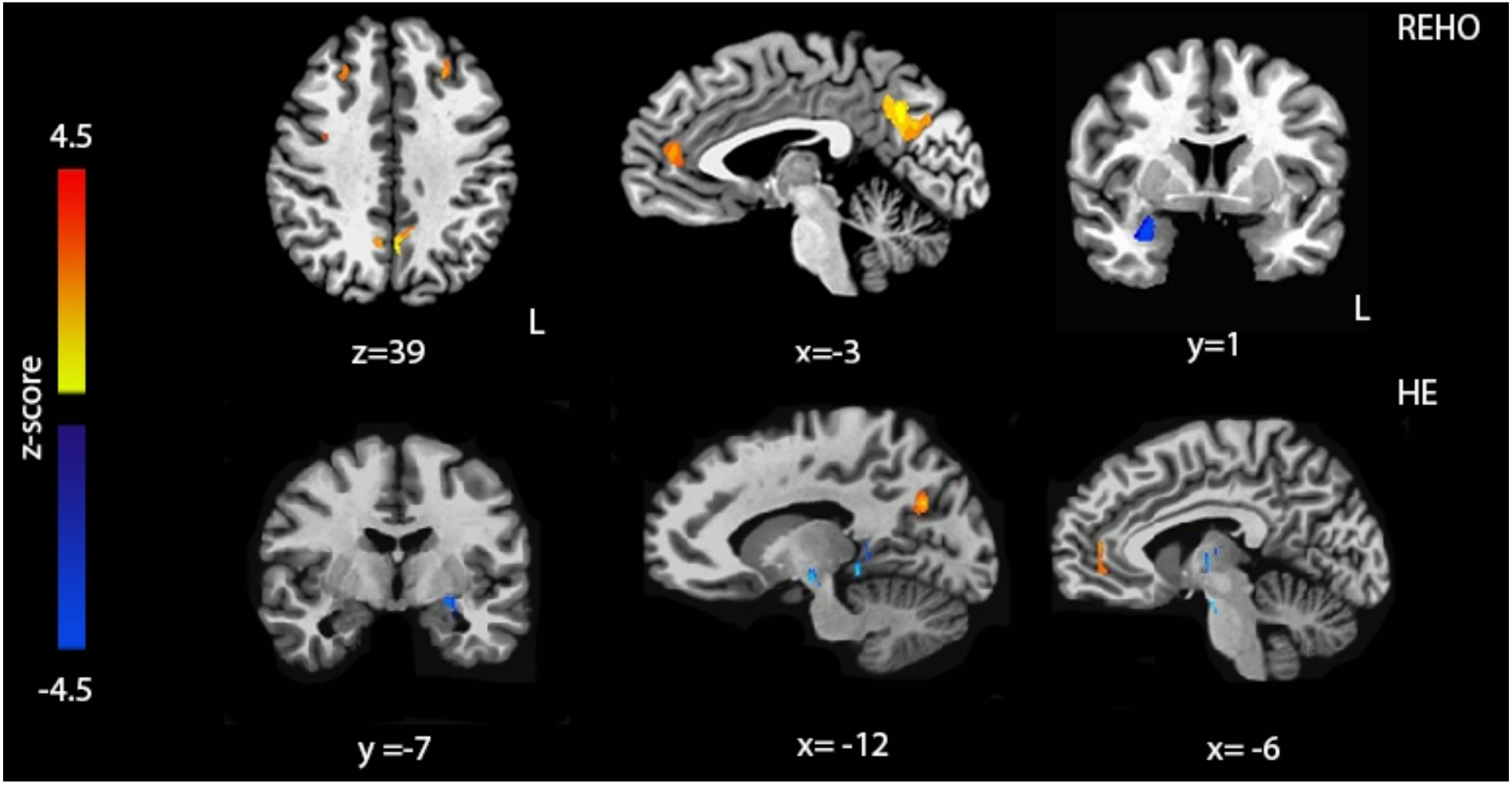
REHO
4.5
z-score
-4.5
z=39
L
x=-3
y=1
L
HE
y =-7
x= -12
x= -6

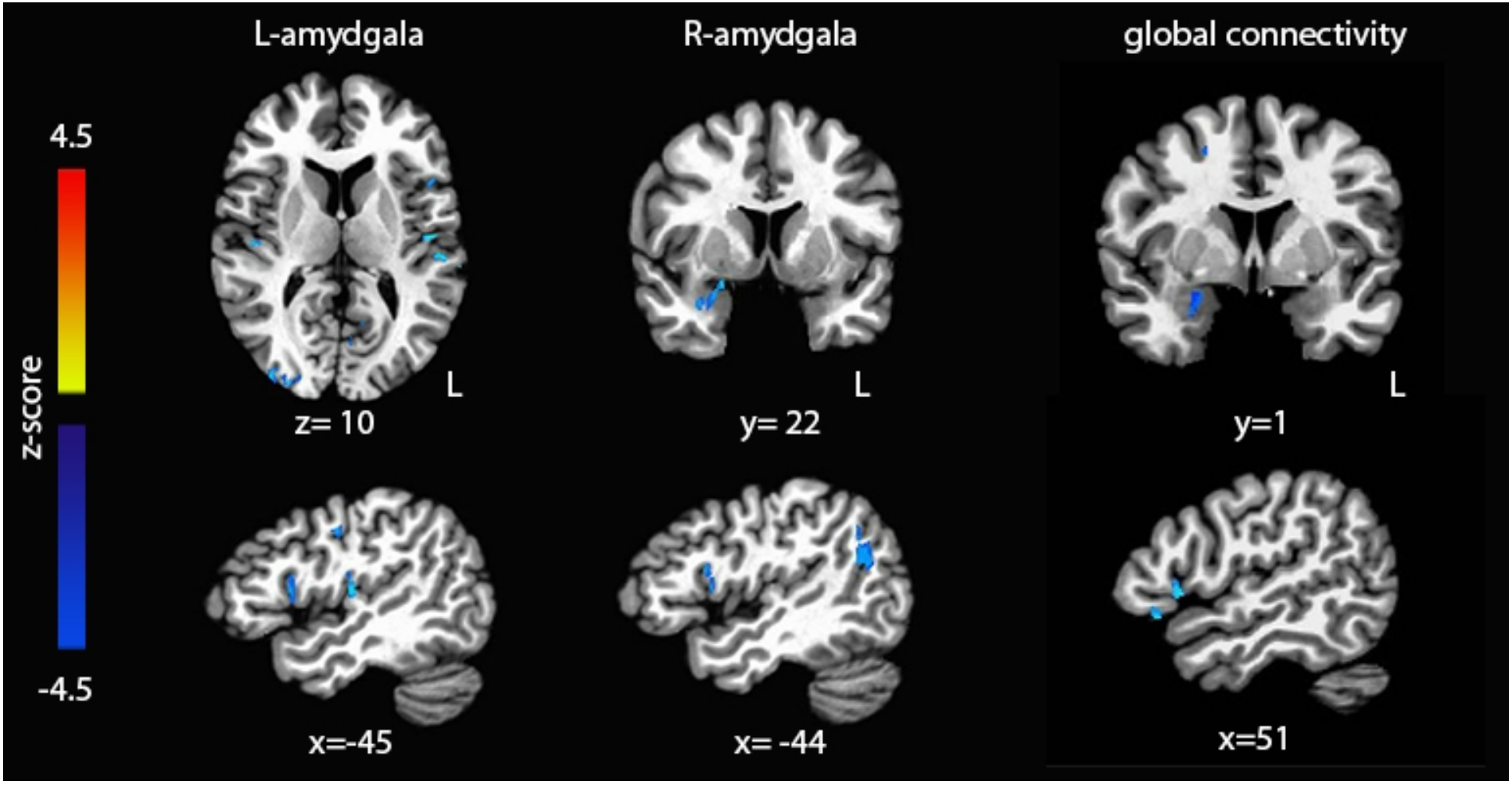
L-amydgala
R-amydgala
global connectivity
4.5
z-score
-4.5
L
L
L
z= 10
y= 22
y=1
x=-45
x= -44
x=51

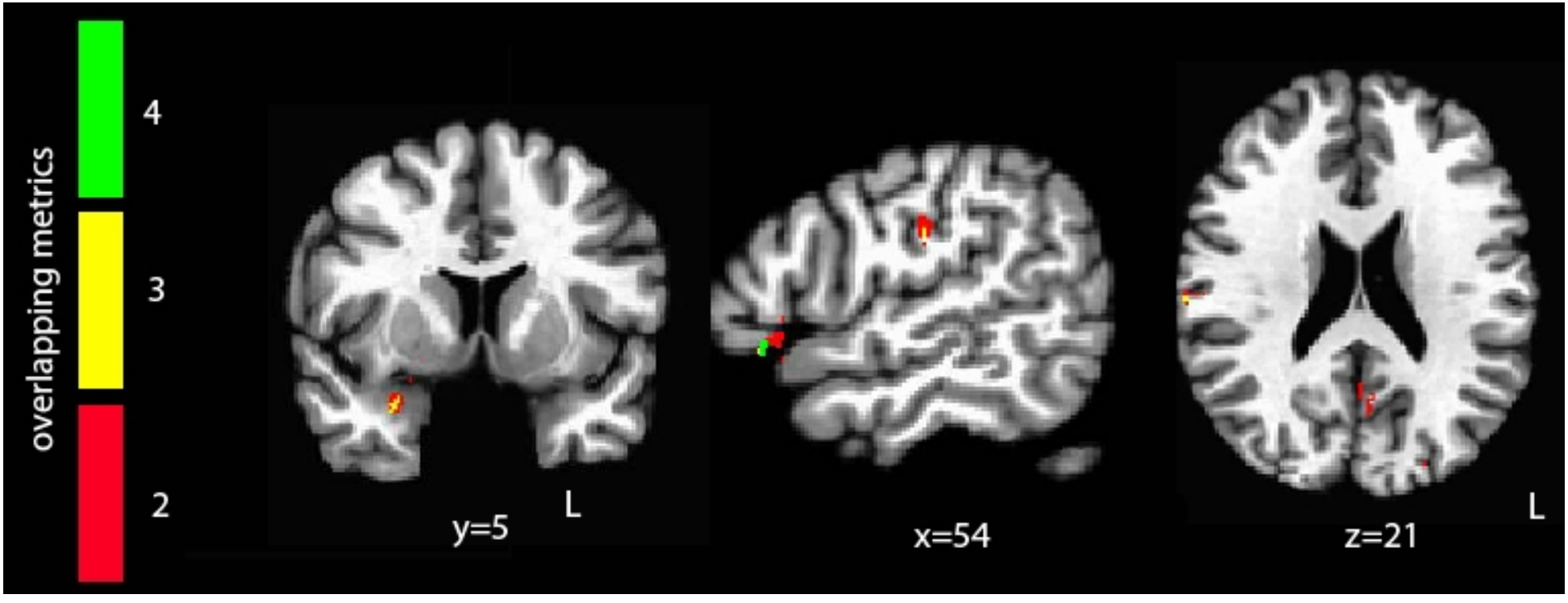
overlapping metrics
4
3
2
y=5
L
x=54
z=21
L

	Volume	Hemi-sphere	Region	center of mass			peak			Z score
				x	y	z	x	y	z	
ALFF										
	592	L	PCC/precun	-2.3	-58.8	29.6	-1.0	-56.0	44.0	3.14
	192	R	ACC	-6.7	41.6	-0.8	-6.0	41.0	2.0	2.94
	163	L	MFG	2.9	-20.6	44.2	1.0	-19.0	47.0	2.65
	95	L	IPL	-31.6	-59.0	32.6	-33.0	-59.0	31.0	2.86
fALFF										
	577	R	IFG	52.7	20.2	1.2	55.0	19.0	-2.0	-3.34
	474	R	IPL	58.9	-17.1	19.8	62.0	-21.0	21.0	-3.08
	411	L	precuneus	-22.6	-80.5	26.5	-27.0	-80.0	25.0	-3.36
	241	R	thalamus	10.1	-17.9	0.6	6.0	-18.0	4.0	-2.78
	228	R	precuneus	23.5	-58.2	47.2	24.0	-58.0	46.0	-4.05
	207	R	fusiform gyr	25.5	-49.9	-8.7	21.0	-56.0	-12.0	-2.72
	173	L	SFG	-26.4	32.7	30.0	-28.0	36.0	31.0	3.71
	153	L	PCC/precun	-1.5	-55.2	19.5	-1.0	-55.0	21.0	3.84
	141	R	IFG	52.1	28.3	0.5	52.0	28.0	2.0	-3.74
	129	R	SFG	24.7	61.0	16.0	23.0	62.0	17.0	-3.84
	119	R	cingulate gyrus	5.9	-24.8	41.1	6.0	-24.0	41.0	-3.20
	114	L	MidFG	-25.4	48.1	12.2	-25.0	51.0	13.0	3.29
	114	L	SPL	-24.9	-55.0	51.7	-25.0	-56.0	55.0	-3.60
	102	R	IPL	61.8	-28.7	27.8	62.0	-28.0	27.0	-3.77
	102	R	cuneus	3.8	-76.7	31.1	2.0	-79.0	29.0	-2.77
	100	R	IPL	37.5	-32.1	42.4	40.0	-33.0	45.0	-4.07
REHO										
	1597	R	amygdala	24.0	-3.7	-16.1	21.0	-7.0	-21.0	-3.16
	1103	L	precuneus	-4.3	-60.4	29.3	-2.0	-60.0	33.0	2.98
	459	L	SFG	-14.2	55.4	22.9	-13.0	56.0	21.0	4.02
	394	R	MidFG	-25.3	29.6	33.2	-22.0	23.0	40.0	2.77
	269	L	fusiform gyr	42.4	-51.1	-9.8	42.0	-50.0	-10.0	4.21
	269	R	MFG	-1.8	44.0	13.4	-0.0	46.0	13.0	3.41
	245	R	IFG	23.0	16.9	-14.2	26.0	19.0	-17.0	-2.79
	235	L	precuneus	8.5	-57.0	34.8	7.0	-56.0	37.0	3.19
	175	R	MidFG	24.1	28.4	34.9	24.0	28.0	36.0	2.86
	162	R	IFG	53.1	18.3	-4.4	55.0	19.0	-2.0	-3.02
	148	L	MidTG	-64.4	-18.6	-7.4	-63.0	-18.0	-6.0	2.88
	139	L	STS	48.0	-45.4	11.3	48.0	-46.0	11.0	3.84
	135	R	STS	36.5	15.8	-18.4	40.0	19.0	-19.0	-2.80
	123	L	precuneus	-29.2	-59.2	28.5	-28.0	-61.0	31.0	2.74
	111	L	ACC	4.6	-3.3	-2.2	4.0	-2.0	0.0	-3.10
	98	L	preCG	33.0	-4.9	33.2	33.0	-4.0	38.0	2.99

	96	R	MidFG	-38.1	17.0	27.6	-39.0	18.0	29.0	3.02
HE										
	282	R	IPL	-58,4	28,6	21,8	-55	28	18	-4.21
	174	L	amygdala	22,9	5	-8,5	22	5	-8	-3.01
	155	L	precuneus	12,2	64,6	26,1	11	67	26	3.86
	139	L	IFG	31,4	-3,8	-10,4	34	-5	-8	-3.04
	138	L	paraHip	20,4	27,1	-4,6	21	26	-6	-3.15
	135	L	paraHip	14,2	34	-6,2	13	34	-6	-2.91
	132	L	paraHip	9,3	38,6	2	8	41	0	-3.11
	118	R	midTG	-50,5	-9,5	-16,9	-51	-9	-19	-3.48
	118	R	TTG	-59,7	15,4	12	-60	16	12	-3.20
	108	R	OFG	-16,6	-10,4	-13,3	-19	-4	-10	-3.03
	105	R	STS	-61,1	22,2	12,8	-61	21	12	-3.57
	104	L	thalamus	3,7	12,8	8,2	3	14	8	-3.32
	94	L	ACC	6,7	-43,3	5,6	6	-44	11	3.25

Volume	Hemi-sphere	Region	center of mass			peak			z score
			x	y	z	x	y	z	
global connectivity									
174	R	amygdala	26.5	2.0	-18.2	22.0	-0.0	-14.0	-2.56
113	R	IFG	50.4	15.5	4.4	52.0	15.0	2.0	-3.01
104	L	lingual gyr	-15.3	-50.6	-6.9	-14.0	-52.0	-6.0	-2.62
96	R	IFG	48.5	17.3	-9.1	49.0	18.0	-8.0	3.13
96	R	MidFG	22.7	-4.7	45.4	23.0	-9.0	46.0	-2.56
95	R	IFG	53.1	23.7	-4.2	53.0	21.0	-4.0	-2.57
FC Left Amygdala									
350	R	SMG	57.6	-18.9	26.4	57.0	-18.0	29.0	-3.62
348	R	MOG	39.9	-79.2	-0.7	38.0	-80.0	-1.0	3.52
325	L	lingual gyrus	-2.6	-73.4	1.6	-1.0	-77.0	-2.0	2.87
294	R	MOG	26.0	-87.3	12.6	21.0	-85.0	19.0	3.65
209	R	cuneus	-17.8	-89.0	21.9	-16.0	-89.0	25.0	-3.68
182	R	fusiform	23.1	-56.9	-10.9	25.0	-60.0	-11.0	3.72
167	R	preCG	-58.1	-3.1	21.3	-61.0	-7.0	16.0	3.63
159	R	IFG	24.8	30.3	-9.5	25.0	31.0	-9.0	-3.97
148	R	temporal pole	48.5	17.4	-8.8	49.0	18.0	-9.0	-3.99
137	L	amygdala	-27.9	-8.8	-10.6	-28.0	-9.0	-9.0	-3.98
136	L	insula	-44.2	-14.5	11.7	-45.0	-15.0	10.0	-3.53
136	R	SMG	56.8	-38.0	22.4	59.0	-38.0	23.0	-3.36
128	R	STS	43.2	-18.1	10.8	46.0	-19.0	7.0	-3.98
123	L	IFG	-45.1	12.3	9.2	-46.0	14.0	11.0	-2.98
122	L	lingual gyrus	-11.0	-59.7	1.6	-11.0	-60.0	-2.0	-3.24
118	R	IFG	45.3	30.9	-9.4	44.0	34.0	-10.0	-4.00
117	L	SOG	-22.7	-80.3	22.4	-23.0	-78.0	25.0	-3.00
117	R	IPL	39.8	-36.1	47.2	41.0	-37.0	50.0	-3.10
116	L	preCG	-45.9	-8.6	37.1	-44.0	-9.0	38.0	-3.69
115	L	STS	-59.4	-27.1	16.2	-59.0	-27.0	17.0	-3.63
114	L	insula	-34.2	16.2	-0.1	-34.0	16.0	0.0	-4.05
114	L	STS	-50.8	-25.1	9.9	-52.0	-25.0	10.0	-3.27
112	R	midOG	35.3	-85.0	10.0	36.0	-85.0	10.0	-4.83
105	R	SMG	31.7	-36.7	38.5	32.0	-38.0	40.0	-3.11
105	L	SPL	-24.7	-42.9	50.1	-25.0	-43.0	55.0	-3.33
102	R	postCG	57.7	-9.9	27.4	59.0	-9.0	24.0	-3.53
99	R	IFG	33.7	26.4	-14.3	32.0	24.0	-14.0	-3.37
99	R	MTG	41.1	-64.7	-1.6	41.0	-65.0	-1.0	-4.08
95	R	amygdala	16.9	-7.5	-12.5	17.0	-7.0	-8.0	-3.31
FC Right									

Amygdala									
	882	L	angular gyrus	-43.2	-56.8	24.7	-41.0	-56.0	26.0	-4.18
	402	L	MTG	-51.7	-49.6	19.5	-53.0	-51.0	20.0	-3.28
	314	R	angular gyrus	41.3	-53.9	34.7	41.0	-57.0	34.0	-3.53
	272	R	amygdala	27.0	3.3	-17.5	21.0	5.0	-12.0	-3.08
	163	R	cingulate	-1.1	-26.8	36.8	-1.0	-25.0	35.0	-3.53
	151	L	STS	-37.3	-71.7	21.6	-35.0	-70.0	22.0	-3.54
	141	R	MorG	3.9	60.5	1.0	3.0	59.0	3.0	-2.88
	136	L	MTG	-40.8	-64.0	16.1	-42.0	-64.0	15.0	-3.42
	133	R	hyppocampus	19.6	-16.3	-10.5	20.0	-16.0	-11.0	-3.72
	125	R	IFG	54.9	20.9	0.6	56.0	19.0	3.0	-3.50
	119	L	IFG	3.9	-74.6	31.9	4.0	-76.0	32.0	-3.62
	118	R	precuneus	-44.8	10.8	15.0	-46.0	10.0	17.0	-3.23
	113	L	insula	-25.0	8.3	-9.1	-26.0	8.0	-10.0	-3.06
	103	R	MTG	65.8	-26.2	-7.7	65.0	-26.0	-8.0	-3.54
	99	R	MOG	-2.9	17.4	46.8	-2.0	17.0	46.0	-3.43
	98	R	SMG	32.2	-67.3	30.5	31.0	-67.0	31.0	-3.54

Volume	Hemi-sphere	Region	peak			metrics influenced in the cluster						FC amygdala	
			x	y	z		ALFF	fALFF	REHO	HE	GC	L	R
283	L	precuneus/ PCC	-2.6	-58.4	24.8	2	X		X				
234	R	amygdala	27.2	1.1	-18.2	4			X		X	X	X
158	R	IFG	51.8	19.9	-5.6	4		X	X		X		X
125	L	MidFG	-25.4	31.0	29.0	2		X	X				
117	R	preCG	55.3	-18.9	25.6	3		X		X		X	
shared presence in the common clusters							1	3	4	1	2	2	2

Highlights

Neuroticism (NE) can be associated with stable Restig State (RS) features,

Several metrics have been used to describe RS, yielding to inconsistent results.

Different metrics portrait different RS properities

Despite regional similarities NE affects different metrics, in different ways.

Multiparametric approach is needed for the characterization of psychological traits.